Enhanced Knowledge in Sciences and Technology Vol. 2 No. 2 (2022) 176-185

EKST

Homepage: http://publisher.uthm.edu.my/periodicals/index.php/ekst
e-ISSN : 2771-6385

Reduced Graphene Oxide Prepared by Hydrothermal Method as Microwave Absorber Filler

Nurul Haliza Hashim[1], Fahmiruddin Esa[1]*,

[1]Department of Physics and Chemistry
Universiti Tun Hussein Onn Malaysia, Pagoh, 84600, MALAYSIA

*Corresponding Author Designation

DOI: https://doi.org/10.30880/ekst.2022.02.02.019
Received 02 January 2022; Accepted 30 January 2022; Available online 23 November 2022

Abstract: Reduced graphene oxide (RGO) provides excellent electrical conductivity due to hybridized energy bonding. Despite previous works, the reduction of RGO is mostly employed the hazardous agents. However, it has been demonstrated that supercritical water may act as reducing agent for RGO under hydrothermal conditions, offering a new and "green" route. In this work, RGO was synthesized at different pH values; 4, 7 and 11. The morphological structure of the RGO reveals that it has a sheet and stacks, with pH 11 having the fewest stacks. The fingerprint of the RGO was developed by functional group observation. The lateral dimensions of graphene sheet were estimated by dynamic light scattering (DLS) technique, which indicates lower in size, 355.5 nm for higher pH value. Permittivity value of 4%-RGO/epoxy composite almost similar and stable at 5 GHz and above. The composite was later designed as planar absorber and simulated at various thickness via free space technique. Major absorption is observed at the bandwidth of 1.88 GHz for 10 mm thickness. The most minimum return loss (RL) is -22 dB indicating that the thickness is comparable with quarter lambda of the resonance frequency. Therefore, the composite is suitable to be used as microwave absorber at the respective loading percentage of filler, thickness and frequency range.

Keywords: Reduce Graphene Oxide, Microwave Absorber, Return Loss.

1. Introduction

Nowadays, microwaves are widely utilized in homes, communications, enterprises, medical, military institutions and they contribute significantly to the evolution of human civilization. EM radiation absorbers are distinguished by their excellent permittivity and electric permeability [1]. In these recent years, there has been a surge in interest in the study of microwave electromagnetic inference (EMI) [2]. In order to solve the EMI issues and the detrimental effects of EMI radiation on humans, much research has been conducted to develop innovative materials with efficient microwave absorption properties and great EMI shielding capabilities [3].

Corresponding author: fahmir@uthm.edu.my

Electromagnetic wave (EM) radiation protection is increasingly important with the rapid advancement of 5G and Internet of Things (IoT) technologies. EM shielding is a typical EM radiation protection technology that uses metal-based or carbon-based films/composites to cover objects that can reflect EM waves [4]. Shielding functional devices based on reduced graphene oxide (RGO) composites, such as RGO composite sheets [5] have recently been disclosed. The fundamental reason for employing graphene-based materials for EM shielding is that graphene has both a high carrier mobility and an electrical conductivity [6], which makes it an excellent choice for EM shielding.

Graphene oxide (GO) is a graphene derivative material with hydroxyl, epoxide and carbonyl groups functionalized on the graphene sheet layer [7]. Furthermore, RGO can be produced in vast amounts at a minimal cost. On the other hand, many reports are discussing the reduction of graphene oxide by using hazardous reducing agents' hydrazine in each case [8]. The use of hazardous is possibly the most well-known procedure in this context, despite the fact that its high toxicity makes the exploration of new environmentally friendly methods worthwhile [9]. Besides, the use of supercritical water as a reducing agent for graphene under hydrothermal conditions has recently been demonstrated, paving the door for a novel and environmentally friendly method of graphene production [9].

To our knowledge, several studies reported of RGO using chemical reducing agent, high temperature or combination of both chemical and high temperature. The uses of hazardous hydrazine are not environmentally friendly method and bring about the aggregation of samples. Hence, it is worthwhile to explore an environment friendly and simple preparation method. In this research, we provide a new insight into this hydrothermal technique by investigating the impact of pH on the synthesis of RGO. We will describe the chemical nature of the resulting species on the basis of the collective employment of Field Emission Scanning Electron Microscope (FESEM), Malvern Zetasizer Nano particle analyzer, and Fourier Transform Infrared (FT-IR). The final goal is that estimating the range of values for the relative permittivity of RGO with the use of a vector network analyzer. To this end, a microwave absorber filler using RGO's permittivity is designed and simulate a broad absorber using CST Microwave Studio.

2. Methodology

2.1 Materials

Graphene oxide powder was bought from SkySpring Nanomaterials. Ethanol and sodium hydroxide were purchased from Merck.

2.2 Sample preparation of RGO

As a standard procedure, RGO was synthesized by dispersing 1.0 g of GO powder in 150 ml of deionized water. The GO suspension was sonicated in 30 minutes and swirled for another 30 minutes. Dropwise additions of 1.0 M NaOH was made to the suspension until the pH of the solution reached 4, 7 and 11 under constant stirring. Hydrothermal treatment of RGO dispersion in Teflon line autoclave was performed at 180℃ for 8 hours. Ethanol was used to centrifuge the final product for several times. Then, it was dried for 24 hours at 100℃ in an oven. All the samples after hydrothermal process were identified and labelled as RGO-A (acidic, pH 4), RGO-N (neutral, pH 7) and RGO-B (basic, pH 11).

2.3 Material characterization

RGO powders obtained through hydrothermal synthesis were palleted for 3 minutes using a hydraulic pressure machine at 1.4 tons of pressure. Field emission scanning electron microscope (FESEM) with EDS (FEI VERSA 3D) was used to study the role played by the PH during the hydrothermal reduction of RGP on the morphology and structure of the obtained RGO sheets. The IR spectrum of RGO powder was taken using a FTIR spectroscopy (Perkin Elmer Spectrum 100) in the 450 cm^{-1} – 4000 cm^{-1} wavenumber range to examine the oxygen-containing functional group. Lateral dimension of RGO sheet and its particle size were measured by zeta potential meter (Malvern Zetasizer

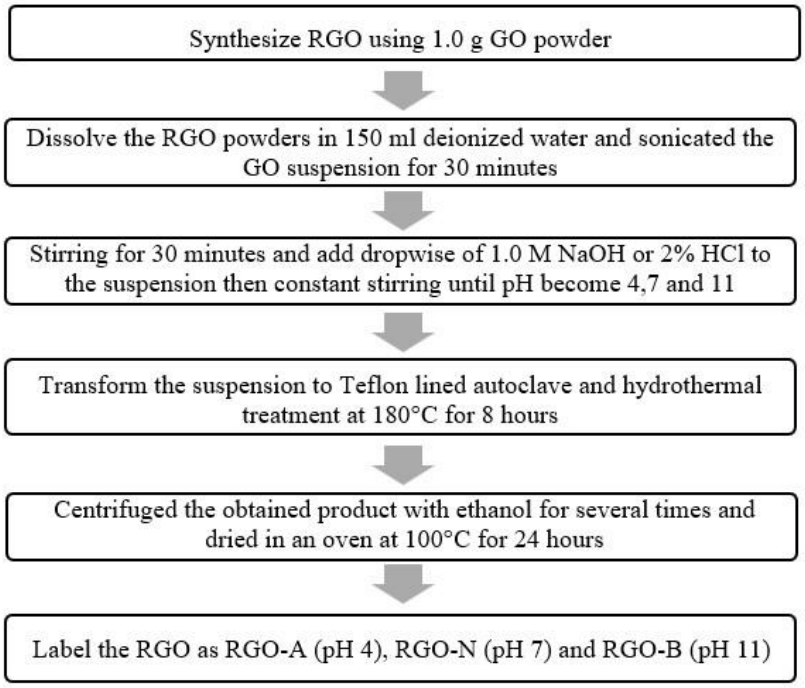

Figure 1: Flow chart of preparation RGO by hydrothermal method

Nano ZS) and the average particle size of particles was measured by dynamic light scattering technique. RGO/epoxy composite was later prepared with 4% loading of RGO dispersed inside epoxy as matric host. The mixture was poured into toroidal shaped mold with outer and inner diameter of 7 mm and 3 mm, respectively. The cast composite was fixed into coaxial airline for scattering parameter (S-parameter) measurement; reflection (S_{11}) and transmission (S_{21}) coefficients using Agilent E5071C network analyzer at the frequency range of 1 kHz – 9 GHz. The raw data of transmission (S_{21}) coefficient for each composite sample was used in transmission phase shift equation for permittivity calculation. The equation can be expressed explicitly as [10]:

$$\varepsilon'_r = \frac{1}{k_o^2}\left\{\left(\gamma_o + \frac{\varnothing_{21}^A - \varnothing_{21}^s}{d}\right)^2 + \left(\frac{\pi}{b}\right)^2 - \alpha^2\right\} \qquad \textit{Eq. 1}$$

$$\varepsilon''_r = \frac{2\alpha}{k_o^2}\left(\gamma_o + \frac{\varnothing_{21}^A - \varnothing_{21}^S}{d}\right) \qquad \textit{Eq. 2}$$

where $k_A = 2\pi f/c$ is the propagation constant of free space (c = 2.99792458 ms^{-1}); b is the width of the aperture of the waveguide, respectively; d is the thickness of the filled sample [15]. The $\varnothing_{21}^A - \varnothing_{21}^S$ in Eq. (1) and Eq. (2) are the measured phase shift of the transmission coefficient in the air (without sample) and the sample respectively. Besides, symbol α is the dielectric attenuation constant for the sample (-1.1512m).

3. Results and Discussion

3.1 Morphology analysis using FESEM

The surface morphologies of RGO were studied using FESEM images. These images were used to analyse the influence of the medium's pH on the morphology of the RGO samples. To emphasis this facts, FESEM images of the RGO at the various pH level are display in Figure 2. These figures clearly indicate that each of the RGOs are curved and wrinkled resulting from the reduction and removal of

functional groups in the graphitic lattice [11]. At highly acidic conditions (pH 4), it is easy to find broken sheets while under basic conditions resulting the less broken sheet. These defects' structure hinders the graphene sheets from creating stacked layers between graphene sheet layers [11] and agglomeration of the sheets due to producing a repulsion between the individual layers [12]. Additionally, its curved shape endows RGO with a mesoporous character, which traps carbon dioxide gas released during hydrothermal reactions.

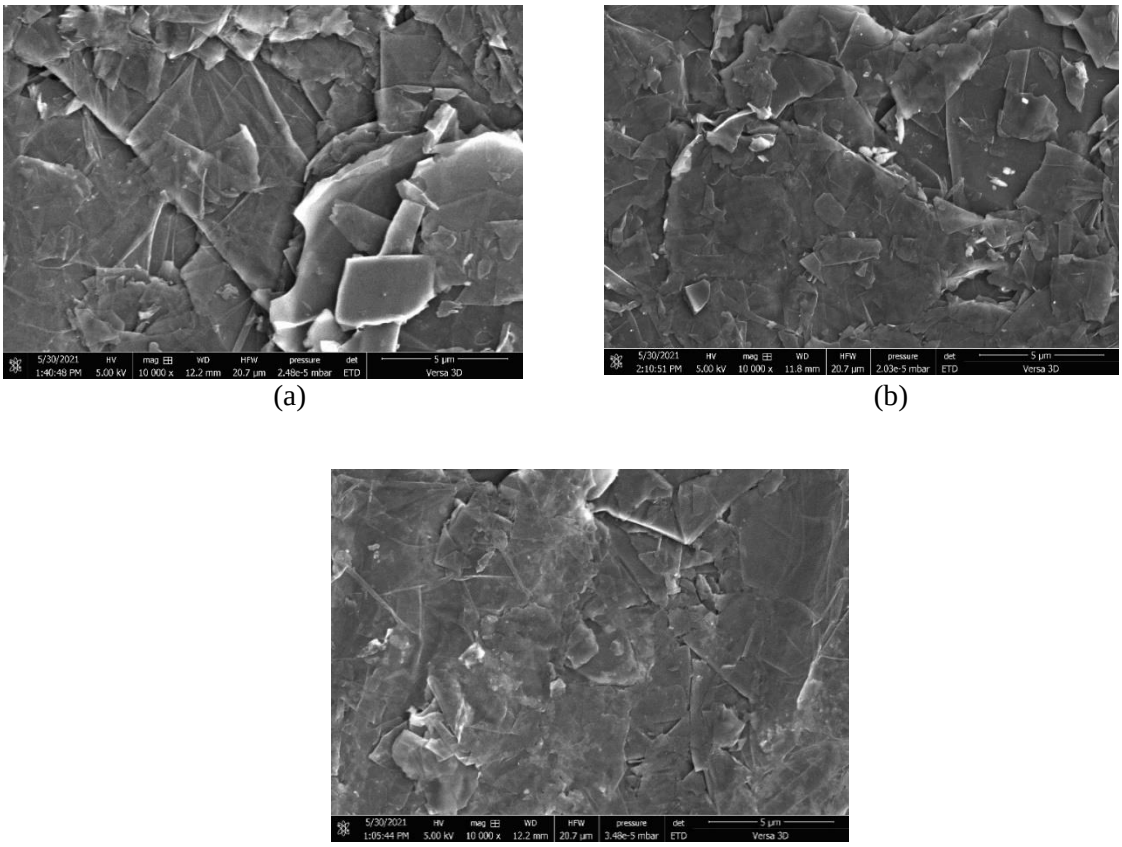

(a) (b)

(c)

Figure 2: FESEM images of (a) RGO-A, (b) RGO-N and (c) RGO-B

3.2 Functional group analysis using FTIR

FTIR spectroscopy was utilized to examine the oxygen-containing functional group in the carbon lattice. Several characteristic modes corresponding to oxygen-containing functional groups were found in each spectrum. Figure 3 depicts the FTIR spectra of RGO samples obtained at pH values of 4, 7, and 11. The IR peaks of RGO samples has the characteristic peaks at 667 cm^{-1} and 868 cm^{-1} representing the C-H bending vibration [7] and 1740 cm^{-1} corresponding to the C=O stretching [13]. Two more peaks placed at around 1047 cm^{-1} and 1217 cm^{-1}. These peaks can be associated to C-O stretching vibration [13]. Next, the hydroxyl groups give rise to the peaks at 1365 cm^{-1}, 2661 cm^{-1} and 225 cm^{-1}. Additional peaks at 2300 $cm^{-1}$are associated with the presence of carbon dioxide molecules emitted by the RGO [7]. All of these distinctive peaks associated with RGO samples are most likely.

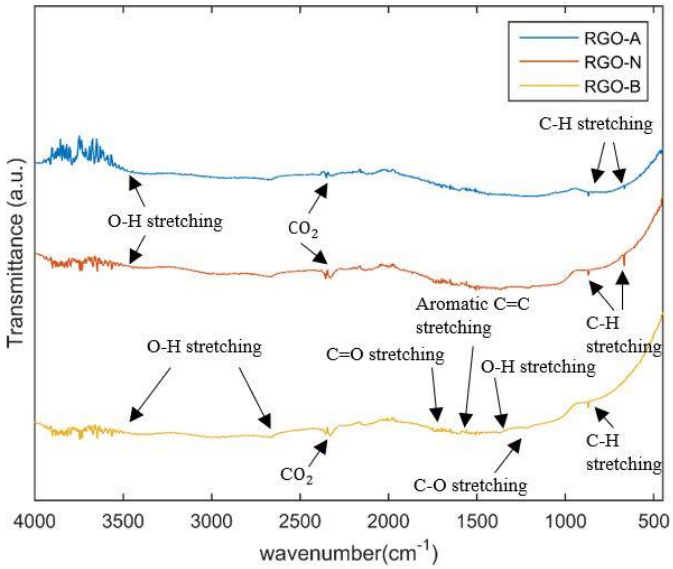

Figure 3: FTIR spectra of RGO-A (pH 4), RGO-N (pH 7) and RGO-B (pH 11)

3.3 Malvern Zetasizer Nano Zs

Dependent on the particle movement in liquid, dynamic light scattering (DLS) is a good technique for measuring the size of lateral dimension as well as its particle size. On the other hand, RGO samples have a considerable length or width ratio (few microns) to thickness (few nanometers) [7]. Thus, DLS pattern of the aforementioned samples are expected to be close to the lateral dimension of the RGO. In Figure 4 depicts the particle size distribution of RGO as assessed by DLS. The particle size distribution in RGO samples was symmetric, with neither negative or positive skewing.

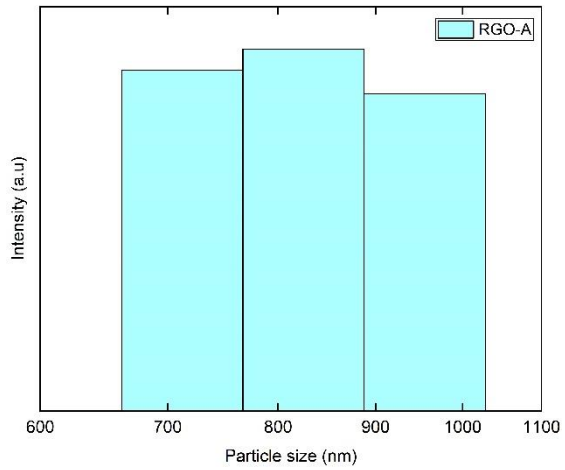

(a)

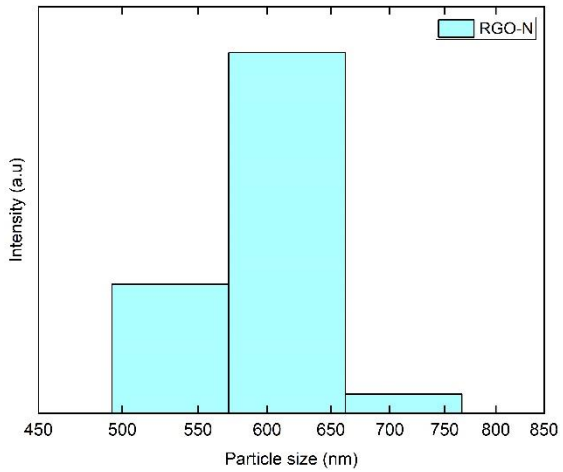

(b)

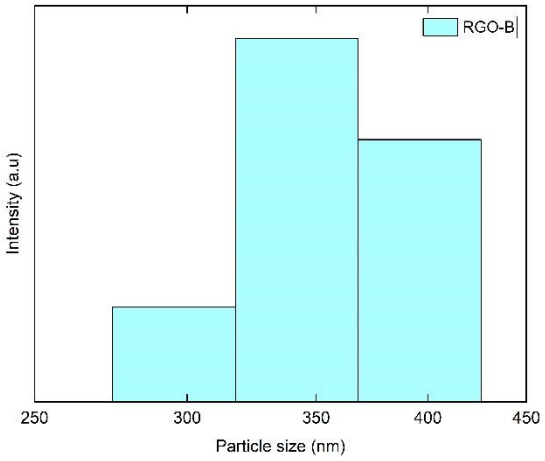

(c)

Figure 4: Particle size distribution of RGO samples at (a) pH 4, (b) pH 7 and (c) pH 11

Table 1: The particle size of RGO samples in various pH values

Samples	pH values	Average particles size (nm)	Range of particle size (nm)
RGO-A	4	763.8	712.4 – 955.4
RGO-N	7	597.5	531.2 – 712.4
RGO-B	11	355.5	295.3 – 396.1

Table 1 shows the Zeta software results for particle size distributions and average RGO values for various pHs. The size distribution of RGO sample at pH 7 ranged from 531.2nm to 712.4nm. When the sample was titrated with NaOH until the higher pH was reached (pH 11), the population was discovered decrease in the range of 295.3nm to 396.1nm. The reason for the decreasing particle size in basic medium could be ascribed to the NaOH acts as hydrogenating agents for graphene oxide and increase the GO's stability [7]. It has also been discovered that NaOH has reliably to remove the oxygen functions from the graphene oxide surface to generate activated graphene sheets [14]. These activated sheets appear to stabilize themselves in the solution by decreasing their effective size. On the other hand, a large size of RGO-A can be seen at 763.8nm. This is due to an increasing of hydrogen ions (H^+) in a solution progressively increase the size of graphene sheet.

3.4 Permittivity of composite

Figure 5 shows the permittivity of epoxy and all 4%RGO/epoxy composites prepared at various pH values. The permittivity almost consistent for all composites throughout the frequency range. Permittivity of pH 7 slightly lower because the sample's length was slightly longer. Fluctuation behavior could be clearly seen especially at lower frequency because of longer sample's length, about 6 mm. However, the fluctional was easily attenuated at higher frequency due to shorter wavelength. The curve of both real and imaginary for all sample decrease as the frequency increase and each of it shows similar variation trends. This phenomenon is known as dipole orientation polarization [14]. Furthermore, interfacial polarization is a key element that contributes to dielectric loss in nanocomposites [14].

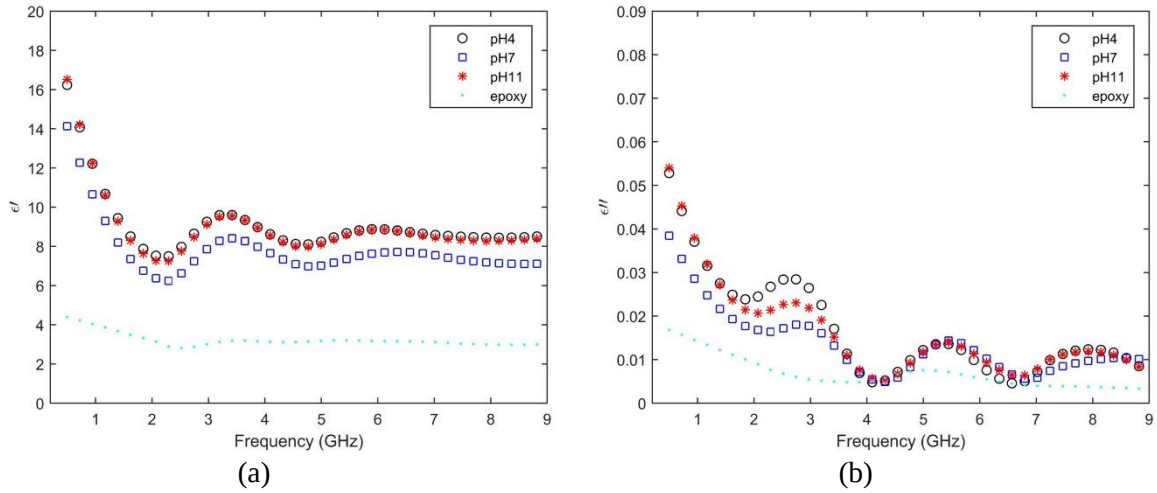

Figure 5: (a)The real part and (b) The imaginary part of permittivity of epoxy and 4%RGO/epoxy composite at various pH values

3.5 CST Simulation analysis

Based on the permittivity result retrieved by transmittion phase shift method (TPS) method, it was found that the data almost stable at 5 GHz until the end of the frequency range. Thus, according to the waveguide and horn standards Institute of Electrical and Electronic Enginners(IEEE), the listed specification below (Table 4.2) is suitable for further investigation as stated in the third objective of this work.

Table 2: The specification of waveguide and horn used in CST simulationn

WR137 Waveguide		Horn Dimension (nm)		
Dimension (nm)	Frequency range (GHz)	A (Overall)	B (Inner)	C (Inner)
34.8488 x 15.7988	5.38 – 8.18	375	170	123

The horn antenna was designed according to the specification as stated in Table 2 and the physical look can be seen in Figure 6(a). The simulation work gave the output of S-parameter as shown in Figure 6(b) where the signal in the frequency range lied under -25 dB, which showed a very good performance of return loss (RL) characteristic. The simulation works were further investigated on the RGO/epoxy composite material with metal-back plate fixed at 300 nm distance from horn aperture (Figure 6(c) and (d)). Several thicknesses of planar RGO/epoxy composites were tested; 6 mm, 10 mm and 14 mm and the simulated return loss (RL) can be seen as in Figure 6(e). The composite width of 10 mm thickness

is the best candidate to be microwave absorber among the others as the absorption bandwidth which is less than -10 dB almost cover more than half of frequency range. The most minimum RL was 22 dB

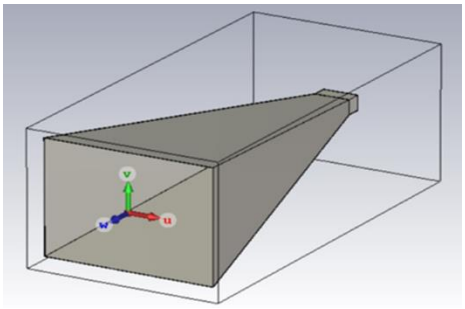

(a)

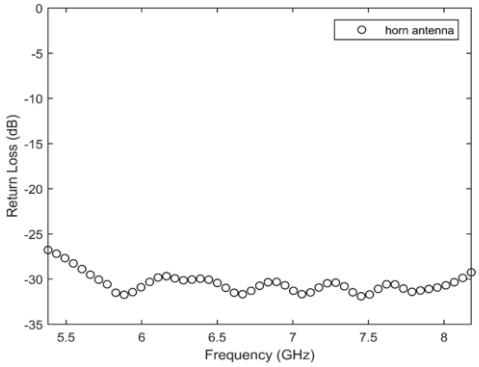

(b)

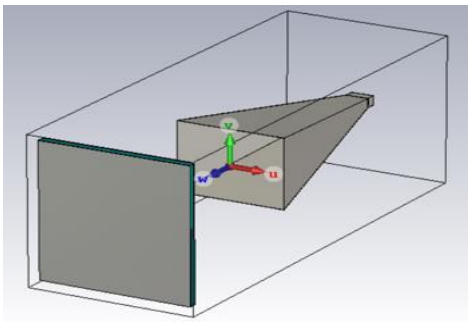

(c)

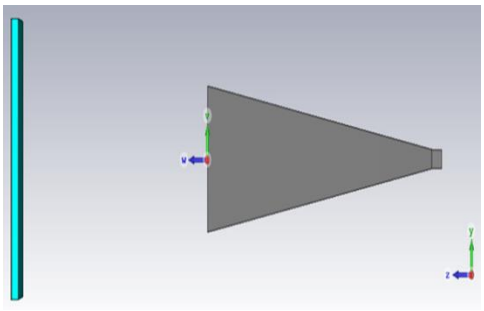

(d)

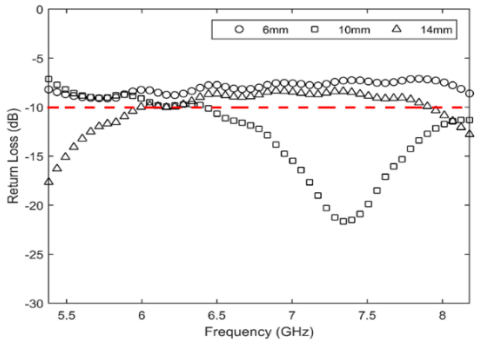

(e)

Figure 6: (a) Perspective view of horn antenna, (b) RL characteristic of horn antenna, (c) Perspective view of RGO/epoxy composite with metal-back plate at 300 mm distance from horn antenna, (d) Side view of RGO/epoxy composite with metal-back plate at 300 mm distance from horn antenna and (e) RL characteristic of planar RGO/epoxy composite at various thickness

The following figures shows the electric and magnetic field distribution at the frequency of 7.34 GHz where the lowest RL occurred. Figure 7(a) shows the side view of electric field at the Y-Z plane cross section where the transverse electric (TE) mode arisen from lower to upper side of longest side wall meanwhile Figure 7(b) is the perspective view of it. Similarly for magnetic field, which shown in Figure 7(c), the perspective view but at X-Z plane cross section because the distribution happened

between the two smallest side walls. Both of the fields are propagating toward the composite along Z-direction.

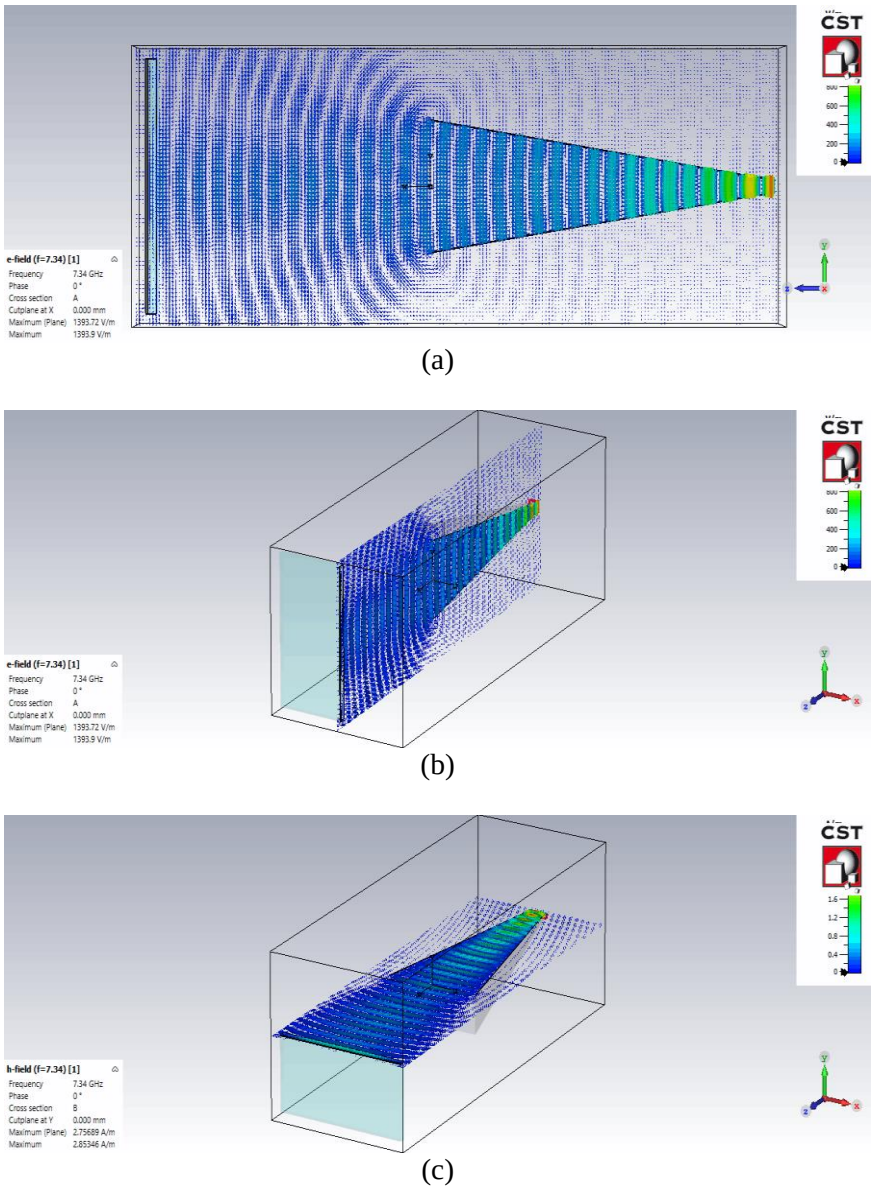

Figure 7: (a)The side of electric field and, (b) the perspective view at the Y-Z plane, (c) the perspective view at X-Z plane

4. Conclusion

In this study, RGO samples was successfully prepared using hydrothermal synthesis in different pH medium (pH 4, pH 7 and pH 11). The FESEM images clearly show the increase of pH values lead to less stacked sheet and tendency to aggregate. The internal structure of the RGO has been additionally studied with FTIR, confirming the fingerprint of functional group. The RGO synthesized in solutions at higher pH values showed the particle size increase (751.1 nm) as compared to the basic medium (344.0 nm) due to the concentration of hydrogen ion increase. Thus, permittivity of 4%-RGO/epoxy almost similar and stable at 5 GHz. Then, the composite was designed as planar absorber and found out the best bandwidth at -22 dB GHz for 10 mm thickness.

5. Acknowledgement

Special thanks from author for Faculty of Applied Science and Technology, UTHM, give full support in terms of instruments. I also extend my thanks to my senior, Yi Lin Chan and Wan Azmafaliyana binti Wan Azmi for the help especially sharing their past research. Then, also thank to my fellow friend to Siti Umairah binti Nasir and Mohamad Aiman bin Manah for support me in any aspect. Last but not least, I would like to thanks to my family for their support and encouragement.

References

[1] Tchouank Tekou Carol T. HY Hafeez, D. Basandrai, Gopala Ram Bhadu, Sachin Kumar Godara, SB Narang, AK Srivastava. (2019) Electromagnetic interference (EMI) shielding, microwave absorption, and optical sensing properties of BaM/CCTO composites in Ku-band, Results in Physics, 13, 102307.

[2] Huang, L., Chen, C., Li, Z., Zhang, Y., Zhang, H., Lu, J., ... & Zeng, Y. J. (2020). Challenges and future perspectives on microwave absorption based on two-dimensional materials and structures. Nanotechnology, 31(16), 162001.

[3] Ibrahim, I. R., Matori, K. A., Ismail, I., Awang, Z., ...& Ertugrul, M. (2020). A study on microwave absorption properties of carbon black and Ni0. 6Zn0. 4Fe2O4 nanocomposites by tuning the matching-absorbing layer structures. Scientific reports, 10(1), 1-14.

[4] Shahzad, F., Alhabeb, M., Hatter, C. B., Anasori, B., Man Hong, S., Koo, C. M., & Gogotsi, Y. (2016). Electromagnetic interference shielding with 2D transition metal carbides (MXenes). Science, 353(6304), 1137-1140.

[5] Liu, Y., Xu, Z., Zhan, J., Li, P., & Gao, C. (2016). Superb electrically conductive graphene fibers via doping strategy. Advanced Materials, 28(36), 7941-7947.

[6] Smith, A. T., LaChance, A. M., Zeng, S., Liu, B., & Sun, L. (2019). Synthesis, properties, and applications of graphene oxide/reduced graphene oxide and their nanocomposites. Nano Materials Science, 1(1), 31-47.

[7] Zhu, Y., Murali, S., Stoller, M. D., Ganesh, K. J., Cai, W., ... & Ruoff, R. S. (2011). Carbon-based supercapacitors produced by activation of graphene. science, 332(6037), 1537-1541.

[8] Bosch-Navarro, C., Coronado, E., Martí-Gastaldo, C., Sánchez-Royo, J. F., & Gómez, M. G. (2012). Influence of the pH on the synthesis of reduced graphene oxide under hydrothermal conditions. Nanoscale, 4(13), 3977-3982.

[9] You, K. Y., Lee, Y. S., Zahid, L., Malek, M. F. A., Lee, K. Y., Cheng, E. M., & Khamis, N. H. H. (2015). Dielectric measurements for low-loss materials using transmission phase-shift method. Jurnal Teknologi, 77(10).

[10] Bai, Y., Rakhi, R. B., Chen, W., & Alshareef, H. N. (2013). Effect of pH-induced chemical modification of hydrothermally reduced graphene oxide on supercapacitor performance. Journal of power sources, 233, 313-319.

[11] Vermisoglou, E. C., Giannakopoulou, T., Romanos, G., Giannouri, M., Boukos, N., Lei, C., ... & Trapalis, C. (2015). Effect of hydrothermal reaction time and alkaline conditions on the electrochemical properties of reduced graphene oxide. Applied Surface Science, 358, 100-109.

[12] Kuila, T., Khanra, P., Kim, N. H., Lim, J. K., & Lee, J. H. (2013). Effects of sodium hydroxide on the yield and electrochemical performance of sulfonated poly (ether-ether-ketone) functionalized graphene. Journal of Materials Chemistry A, 1(32), 9294-9302.

[13] Ahmad, A. F., Ab Aziz, S., Abbas, Z., Obaiys, S. J., Khamis, A. M., Hussain, I. R., & Zaid, M. H. M. (2018). Preparation of a chemically reduced graphene oxide reinforced epoxy resin polymer as a composite for electromagnetic interference shielding and microwave-absorbing applications. Polymers, 10(11), 1180.

[14] Singh, K., Ohlan, A., Pham, V. H., Balasubramaniyan, R., Varshney, S., Jang, J., ... & Chung, J. S. (2013). Nanostructured graphene/Fe 3 O 4 incorporated polyaniline as a high performance shield against electromagnetic pollution. Nanoscale, 5(6), 2411-2420.